

Algoritmo de Optimización de Mapeo de Media Varianza Aplicado al Despacho Óptimo de Potencia Reactiva

Mean-Variance Mapping Optimization Algorithm Applied to the Optimal Reactive Power Dispatch

DOI: <http://doi.org/10.17981/ingecuc.17.1.2021.19>

Artículo de Investigación Científica. Fecha de Recepción: 13/07/2020. Fecha de Aceptación: 17/02/2021.

Daniel Camilo Londoño Tamayo 

Universidad de Antioquia. Medellín (Colombia)
dcamilo.londono@udea.edu.co

Jesús María López Lezama 

Universidad de Antioquia. Medellín (Colombia)
jmaria.lopez@udea.edu.co

Walter Mauricio Villa Acevedo 

Universidad de Antioquia. Medellín (Colombia)
walter.villa@udea.edu.co

Para citar este artículo:

D. Londoño Tamayo, J. López Lezama & W. Villa Acevedo, “Mean-Variance Mapping Optimization Algorithm Applied to the Optimal Reactive Power Dispatch”, *INGECUC*, vol. 17. no. 1, pp. 239–255. DOI: <http://doi.org/10.17981/ingecuc.17.1.2021.19>

Abstract

Introduction— The optimal reactive power dispatch (ORPD) problem consists on finding the optimal settings of several reactive power resources in order to minimize system power losses. The ORPD is a complex combinatorial optimization problem that involves discrete and continuous variables as well as a non-linear objective function and nonlinear constraints.

Objective— This article seeks to compare the performance of the mean-variance mapping optimization (MVMO) algorithm with other techniques reported in the specialized literature applied to the ORPD solution.

Methodology— Two different constraint handling approaches are implemented within the MVMO algorithm: a conventional penalization of deviations from feasible solutions and a penalization by means of a product of subfunctions that serves to identify both when a solution is optimal and feasible. Several tests are carried out in IEEE benchmark power systems of 30 and 57 buses.

Conclusions— The MVMO algorithm is effective in solving the ORPD problem. Results evidence that the MVMO algorithm outperforms or matches the quality of solutions reported by several solution techniques reported in the technical literature. The alternative handling constraint proposed for the MVMO reduces the computation time and guarantees both feasibility and optimality of the solutions found.

Keywords— Reactive power; metaheuristic techniques; power loss minimization; constraint handling; mean-variance mapping optimization

Resumen

Introducción— El problema del despacho óptimo de potencia reactiva (DOPR) consiste en encontrar la configuración óptima de diferentes recursos de potencia reactiva para minimizar las pérdidas de potencia del sistema. El DOPR es un problema complejo de optimización combinatorial que involucra variables discretas y continuas, así como una función objetivo no lineal y restricciones no lineales.

Objetivo— En este artículo se busca comparar el desempeño del algoritmo de optimización de mapeo de media varianza (MVMO, por sus siglas en inglés) con otras técnicas reportadas en la literatura especializada aplicadas a la solución del DOPR.

Metodología— En el algoritmo MVMO se aplican dos enfoques diferentes de manejo de restricciones: penalización convencional de las desviaciones de las soluciones factibles y penalización por medio del producto de subfunciones que sirve para identificar cuándo una solución es óptima y factible. Se realizan simulaciones en sistemas de prueba IEEE de 30 y 57 barras.

Conclusiones— El algoritmo MVMO es efectivo para solucionar el DOPR. Los resultados evidencian que el algoritmo MVMO supera o iguala a varias técnicas reportadas en la literatura técnica en la calidad de soluciones. El manejo alternativo de restricciones propuesto para el MVMO reduce el tiempo de cálculo y garantiza tanto factibilidad como optimalidad de las soluciones encontradas.

Palabras clave— Potencia reactiva; técnicas metaheurísticas; minimización de pérdidas; manejo de restricciones; optimización de mapeo de media-varianza



I. INTRODUCTION

The Optimal Reactive Power Dispatch (ORPD) is a vital process in the daily operation of power systems. The main objective of the ORPD is the minimization of active power losses, although other objectives have been proposed such as the minimization of the voltage deviation in the nodes and the improvement of the voltage stability limits of the system [1]. These objectives may be achieved by finding an optimal configuration of reactive power sources and other elements in charge of reactive power control. The ORPD involves integer decision variables such as transformers taps and the position or step of the reactive power compensation devices, as well as continuous decision variables such as voltage set points of generators. Furthermore, the mathematical model of the ORPD has non-linear constraints and a non-linear objective function, which makes it a challenging optimization problem. The first attempts to approach these problem are based on conventional optimization techniques such as linear programming [2], mixed integer linear programming [3], quadratic programming [4], dynamic programming [5] and interior point methods [6]. Despite the relative success of such techniques there are still some difficulties associated. The main drawback of conventional optimization techniques lies on the fact that they are often trapped on local optimal solutions given the non-differential non-linear and non-convex nature of the ORPD problem. From the standpoint of mathematical complexity this problem is NP-complete. These type of problems are better handled by metaheuristic techniques.

In the technical literature, different metaheuristic techniques are proposed to address the ORPD problem. In some research [7] the authors propose a Differential Evolution (DE) technique to solve the ORPD problem. DE is a population-based algorithm such as Genetic Algorithms (GA) that implements crossover, mutation, and selection operators. The main difference between DE and GA are the selection and mutation stages. In other [8], the authors present a Chaotic Krill Herd Algorithm (CKHA) to solve the ORPD. This method is described and is based on the behavior of a krill herd when searching food [9]. This metaheuristic technique combines a random and local search to account for diversification and intensification, respectively. Results are presented in the IEEE 30 and 57 bus test systems, comparing the CKHA with other evolutionary optimization techniques. Three objectives are considered independently: minimization of power losses, minimization of voltage drift and improvement of voltage stability. A Particle Swarm Optimization (PSO) is developed in a few studies [10] to solve the ORPD considering voltage control. This last objective is achieved through a continuation power flow and a contingency analysis. other variants of this technique have also been applied, to solve the ORPD such as hybrid PSO [11]; Turbulent PSO [12]; comprehensive learning particle swarm optimization (CLPSO) [13] and Particle Swarm Optimization with an Aging Leader and Challengers (ALC-PSO) [14]. The researchers propose a Gravitational Search Algorithm (GSA) to solve the ORPD [15]. This technique was initially proposed in 2009 [16] and is a swarm metaheuristic inspired in the gravitational law. Some variations of this technique applied to the ORPD are the Improved Gravitational Search Algorithm (IGSA), and the Opposition-based Gravitational Search algorithm (OGSA) [17], [18].

On the other hand, other metaheuristics techniques have been applied to solve the ORPD such as the Firefly Algorithm (FA), Hybrid Firefly Algorithm (HFA) [19], Artificial Bee Colony (ABC) algorithm [20], Seeker Optimization Algorithm (SOA) [21], Biogeography-Based Optimization (BBO) [22], Moth-Flame Optimization (MFO) [23] and Gaussian Bare-bones Water Cycle Algorithm (GBWCA) [24]. A detailed description of all the above techniques is outside the scope of this document [25].

In this paper, several metaheuristic techniques applied to ORPD are compared with an adaptation of the Mean-Variance Mapping Optimization algorithm (MVMO) proposed by the authors. The main contributions of this document are two: 1) a novel adaptation of the MVMO algorithm is implemented to address the ORPD problem; 2) two approaches to handling constraints are developed and compared for the proposed algorithm. Additionally, a comparison with other techniques applied to the ORPD solution is presented. In all cases, results of equal or better quality were found, which shows the applicability and effectiveness of the proposed method.

II. MATHEMATICAL FORMULATION OF THE ORPD

A. Objective Function

The objective function of the ORPD consists on minimizing active power losses as indicated in (1). In this case, N_K , is the set of lines, represents active power losses, g_k , is the admittance of line k (connected between nodes i and j), V_i and V_j are the voltage magnitudes at buses i and j , respectively; finally, θ_{ij} is the angle between buses i and j .

$$\text{Min Ploss} = \sum_{k \in N_K} g_k (V_i^2 + V_j^2 - 2V_i V_j \cos \theta_{ij}) \quad (1)$$

B. Constraints

The constraints associated with the ORPD are given by (2) to (9). Equations (2) and (3) correspond to active and reactive power balance respectively. In this case, N_B , is the set of buses, G_{ij} and B_{ij} are real and imaginary entries of the admittance matrix in position i, j , respectively. P_{gi} and P_{di} are the active generation and demand at bus i , respectively. Finally, Q_{gi} and Q_{di} are the reactive generation and demand at bus i , respectively

$$V_i \sum_{j \in N_B} V_j [G_{ij} \cos \theta_{ij} + B_{ij} \sin \theta_{ij}] - P_{gi} + P_{di} = 0 \quad (2)$$

$$V_i \sum_{j \in N_B} V_j [G_{ij} \sin \theta_{ij} - B_{ij} \cos \theta_{ij}] - Q_{gi} + Q_{di} = 0 \quad (3)$$

Equations (4) to (9) are the inequality constraints of the ORPD. Upper indexes *min* and *max* represent minimum and maximum limits of the corresponding variable. Equation (4) represents voltage limits of generators. In this case, V_{gi} , is the reference voltage magnitude of the i^{th} generator, while N_G , is the set of generators.

$$V_{gi}^{\min} \leq V_{gi} \leq V_{gi}^{\max} \quad i = 1, \dots, N_G \quad (4)$$

Equation (5) represents the limits on tap positions of transformers and N_T is the set of available transformers with on-load tap changers.

$$T_i^{\min} \leq T_i \leq T_i^{\max} \quad i = 1, \dots, N_T \quad (5)$$

Equations (6) and (7) represent the limits of reactive power delivered by capacitor banks and reactors, respectively. In this case Q_{ci} and Q_{Lj} are the reactive power injections of the capacitive bank i and reactor j , respectively. N_C and N_L are the set of capacitors and reactors, respectively.

$$Q_{ci}^{\min} \leq Q_{ci} \leq Q_{ci}^{\max} \quad i = 1, \dots, N_C \quad (6)$$

$$Q_{Lj}^{\min} \leq Q_{Lj} \leq Q_{Lj}^{\max} \quad j = 1, \dots, N_L \quad (7)$$

Equation (8) represents the voltage limits in load buses, where V_{PQi} is the i^{th} load bus and N_{PQ} is the set of load buses.

$$V_{PQi}^{\min} \leq V_{PQi} \leq V_{PQi}^{\max} \quad i = 1, \dots, N_{PQ} \quad (8)$$

Finally, equation (9) represents the apparent power flow limits. In this case S_{ln} represents the apparent power flow in line n and N_n is the number of lines in the system.

$$|S_{ln}| \leq S_{ln}^{max} \quad n = 1, \dots, N_n \quad (9)$$

C. Codification of solutions

The control variables of the ORPD are given by the set points of the generators, the positions of the taps of the transformers and the injections of reactive power provided by the capacitor and reactor banks. Such values are limited by constraints (4) - (7), respectively. The application of these constraints is done directly in the codification of candidate solutions. Each set of variables starts randomly within their respective limits. For example, generator voltages are considered within the range $[V_{g1}^{min}, V_{g1}^{max}]$ using fine discretization. In the same way, other limits are considered for the positions of the taps of the transformers, capacitor banks and reactors. Each variable is coded according to the specific data of the system. Fig. 1 represents the codification of a candidate solution

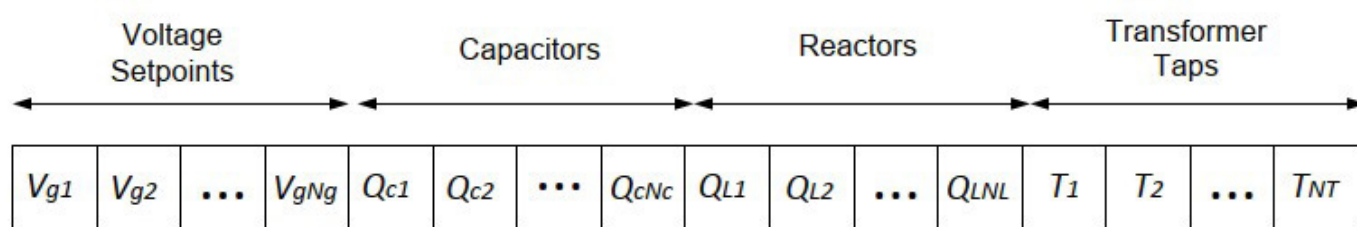


Fig. 1. Codification of candidate solutions.
Source: Autors.

D. Constraint handling of the ORPD

Enforcement of constraints (2) and (3) is given through the solution of a power flow, while the enforcement of constraints (4)-(7) is given through the codification of candidate solutions. Constraints (8) and (9) are handled by penalizing deviations from established limits. In this case, a fitness function labeled as F_1 is defined as the power losses plus penalizations of voltage deviations (VD), and power flow deviations (PFD) as indicated in equations (10)-(12). In this case μ_v and μ_{pf} are the penalization factors for VD and PFD, respectively.

$$F_1 = Ploss + \mu_v VD + \mu_{pf} PFD \quad (10)$$

$$VD = \sum_j \max\{0, (V_j^{min} - V_j)\} + \max\{0, (V_j - V_j^{max})\} \quad (11)$$

$$PFD = \sum_k \max\{0, (S_{lk}^{min} - S_{lk})\} + \max\{0, (S_{lk} - S_{lk}^{max})\} \quad (12)$$

Equation (13) represents an alternative approach to handle constraints within the ORPD, which can also be used as a stopping criterion of the optimization process [25]. The proposed fitness function given by (13) consists on a product of subfunctions with three components: voltage limits in load buses (f_{VN}), power flow limits in branches (f_{CR}) and a goal on total power losses (f_{loss}).

$$F_2 = \left[\prod_{i=1}^{N_L} f_{VN}(i) \right] \left[\prod_{j=1}^{N_K} f_{CR}(j) \right] f_{loss} \quad (13)$$

Each subfunction is designed in such a way that if the corresponding variable is within the specified limits, it returns a value equal to 1; otherwise, its value is less than 1 (Fig. 2).

As regards power losses, a goal is previously defined; then the subfunction is set as indicated in Fig. 2c. Such loss goal is established based on the knowledge of the power system operator. It should be noted that the product of all subfunctions is equal to 1 only if the ORPD problem is feasible (meets all constraints) and optimal (according to a specific objective). This represents an advantage from an optimization point of view, since the value of F_2 can be used as a stopping criterion. More details on the implementation of F_2 within the ORPD problem can be found [26].

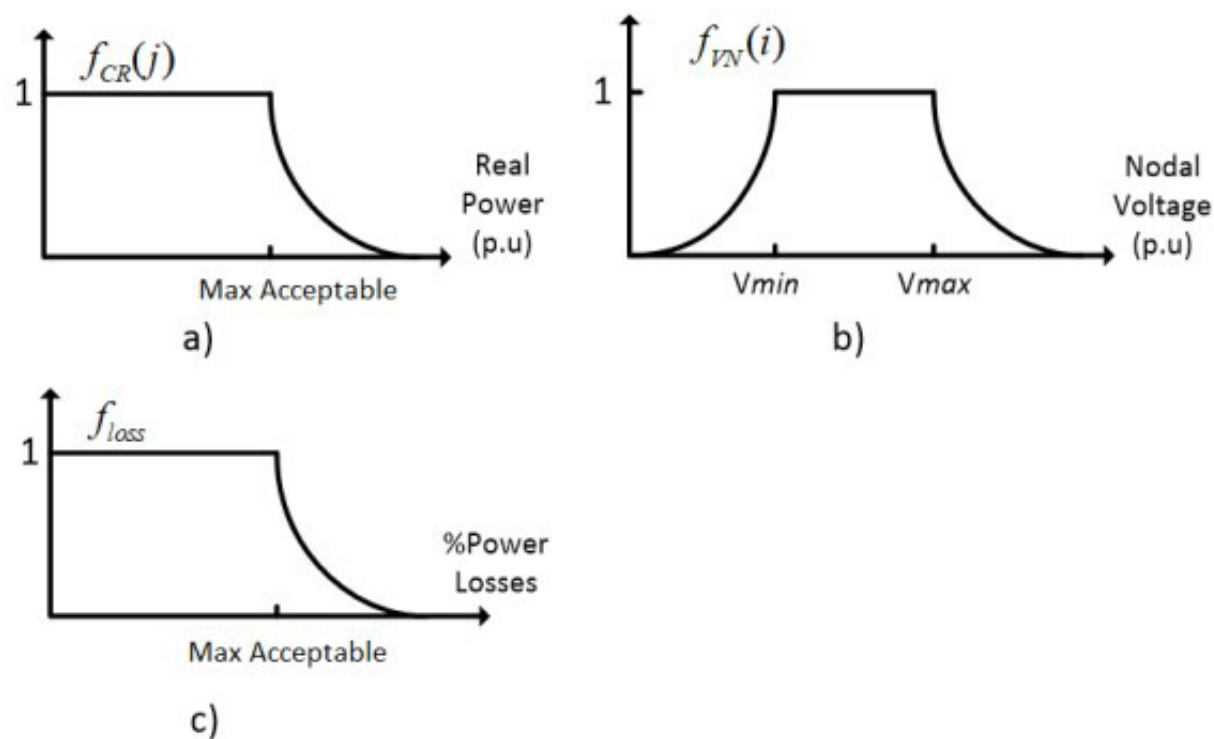


Fig. 2. Subfunctions for: a) Power flow limits; b) Limits on voltage limits in load buses; and c) Limit on power losses.

Source: Authors.

III. METHODOLOGY

The MVMO was initially conceived and developed by István Erlich in 2010 [27]. The basic concept shares several similarities with other evolutionary algorithms; however, its main feature is the use of a special mapping or assignment function, to then apply the mutation to the offspring, based on the mean and variance of the n-best population. The swarm version of this algorithm [28], [29], is implemented in this paper.

As in most evolutionary algorithms, the classic MVMO operates on a set of solutions. The internal search space of all variables within the MVMO is restricted to [0,1]. Therefore, the minimum and maximum limits of the variables must be normalized in this range. In each iteration, it is not possible for any vector solution component to violate the corresponding limits. To achieve this goal, a special mapping function was developed. The inputs to this function are the mean and variance of the best solutions that the MVMO has found. It should be noted that the output of this mapping function will always be within the range [0,1], avoiding the violation of the limits of the variables during the search process. The shape and mapping curves are adjusted according to the progress in the search process and the MVMO updates the candidate solution around the best solution at each step of the iteration [27]. The basic considerations of the classic MVMO are detailed below.

A. Fitness evaluation and constraint handling

The chi-square test is applied for each candidate solution. The feasibility of the solution is verified and a value is assigned to the fitness function. The static penalty approach is used to handle constraints. As the control variables are self-limited, all the dependent variables are restricted by applying the fitness function as indicated in (14) where is the original objective function, n is the number of constraints, β is the order of the penalty term, v_i is the penalty coefficient of the i th constraint and represents the inequality constraints.

$$\min f' = f + \sum_{i=1}^n v_i \max[0, g_i]^\beta \quad (14)$$

B. Improved mapping

The mapping function transforms a randomly generated variable x_1^* with unit distribution to another variable x_i , which is concentrated around the mean value. The new value of the i th variable is determined by (15). Where h_x , h_1 and h_0 are the outputs of the mapping function based on the different inputs given by (16). The mapping function (function h) is parameterized as indicated in (17), where s_1 and s_2 are form factors that allow asymmetric variations of the mapping function.

Finally, the form factor is calculated as indicated in equation (18). In this case, f_s is a scaling factor that allows controlling the search process during each iteration, while \bar{x}_i and v_i are the mean and variance of the solution file, respectively [30].

$$x_i = h_x + (1 - h_1 + h_0)x_i^* - h_0 \quad (15)$$

$$h_x = h(x = x_i^*), h_0 = h(x = 0), h_1 = h(x = 1) \quad (16)$$

$$h(\bar{x}, s_1, s_2, x) = \bar{x}(1 - e^{-x \cdot s_1}) + (1 - \bar{x})e^{-(1-x)s_2} \quad (17)$$

$$s_i = -\ln(v_i)f_s \quad (18)$$

C. Solutions file

This file constitutes the basic knowledge of the algorithm to guide the search. Therefore, the n best individuals that the MVMO algorithm has found are stored in this file. The fitness value for each individual is also saved. The following rules are adjusted to compare the individuals generated in each iteration and the existing archived solutions in order to avoid the loss of high-quality solutions: (i) any feasible solution is preferred over any unfeasible solution, (ii) between two unfeasible solutions, the one with the best objective function is preferred, (iii) between two unfeasible solutions, the one with the lowest fitness value is preferred. The update is only done if the new individual is better than the ones currently on file. Viable solutions are at the top of the file. The feasible solutions are organized according to their physical value. Feasible solutions are organized according to their fitness value and are located at the bottom of the file. Once the file is complete with n feasible solutions, any unfeasible solution candidates cannot be saved in the file.

D. Parents assignment

The first solution positioned in the file (the best so far), named x_{best} , is assigned as the parent.

E. Generation of offspring

Variable selection is done at this stage. The MVMO searches the mean value stored in the solution file to find the best solution only in m selected addresses. This means that only these dimensions of the offspring will be updated, while the remaining $D - m$ dimensions take the corresponding values of x_{best} , where D is the dimension of the problem (number of control variables). Then, the mutation is carried out, for each m dimension selected.

F. Stopping criterion

The MVMO search process stops after a predetermined number of fitness function assessments.

G. *Swarm variant*

In its swarm variant, MVMO starts with n particles. In this case, each particle, or candidate solution, has its own solution file and its mapping function. In the process, each candidate solution executes m steps to identify an optimal set of independent solutions. Subsequently, the particles exchange information. In some cases, some particles are very close to each other, which means that there is redundancy of information. This is solved by discarding the redundant particles. As in the case of PSO, a better local and global solution is defined. The normalized distance between each particle to the best local and global solutions is also calculated.

A particle is discarded from the process if its normalized distance is less than a certain pre-defined threshold. If that threshold is zero, all particles are taken into account throughout the process; otherwise, if the threshold is one, all particles except those of the best overall solution are discarded. Upon independent evaluation, and if the particle is still being considered, the search will be directed towards the global solution by assigning the best global rather than the best local solution, as the parent. The remaining steps are identical to those of the classic MVMO. Fig. 3 shows a flow chart of the implemented MVMO [29], [31].

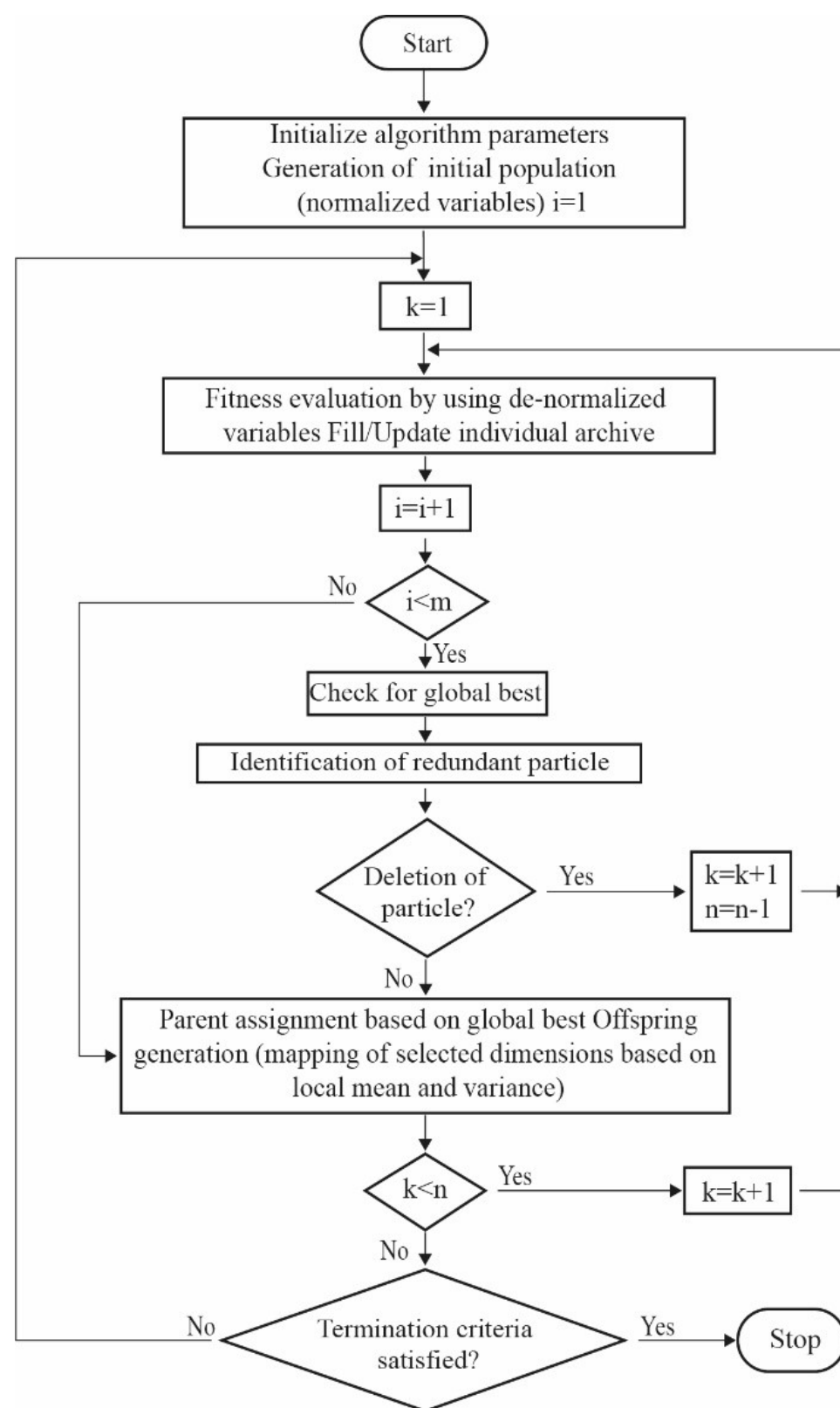


Fig. 3. Flowchart of MVMO algorithm.
Source: [29].

IV. RESULTS

A. Description of the IEEE test systems

To validate the proposed methodology, the IEEE 30 and 57 bus test systems were used [7]. Its main characteristics are indicated in Table 1. For both power systems 100 runs of the algorithm were carried out. For objective function F_1 , the penalty factors $\mu_v = 10\,000$ and $\mu_{pf} = 1\,000$ are used. For the implementation of F_2 , a target power losses for both test systems is considered. Such goal is set based on the results reported in the specialized literature and is indicated in the last row of Table 1.

TABLE 1. MAIN CHARACTERISTICS OF THE TEST SYSTEMS UNDER STUDY.

Characteristic	IEEE-30	IEEE-57
Buses	30	57
Load Buses	24	50
Generators	6	7
Transformers with taps	4	15
Capacitors	9	3
Branches	41	80
Control variables	19	25
Losses (base case) (MW)	5.833	27.864
Goal on losses (MW)	4.480	23.680

B. Results with the IEEE 30-bus test system

In Table 2a, Table 2b, Table 2c and Table 2d, the results obtained with the IEEE 30-bus test system are presented. The data are given in pu considering a base of 100 MVA. A comparison with different metaheuristics techniques applied to the same problem and reported in the specialized literature is presented. To ensure the reproducibility of the results, the specific values of all the control variables are shown in Table 2a, Table 2b, Table 2c and Table 2d. Note that the power losses before optimization are 5.833 MW (Table 1). The best reduction in power losses is obtained through the proposed MVMO algorithm using fitness function F_1 , which results in power losses of 4.5626 MW, which represents a reduction of 21.48% compared to the base case. Note that when applying fitness function F_2 , the MVMO is slightly outperformed by DE and BBO; however, its performance is still superior to that of the other metaheuristics. Fig. 4 allows a quick comparison of the results obtained with different methodologies. It can be seen that the performance of the MVMO is similar to that of MFO, DE and BBO. Fig. 5 and Fig. 6 illustrate the convergence of the proposed approach for fitness functions F_1 and F_2 , respectively. In this case, four runs of the algorithm are randomly selected. Note that regardless of the initial condition, all executions converge to approximately the same value; furthermore, converges to -1, since the problem is fixed for minimization.

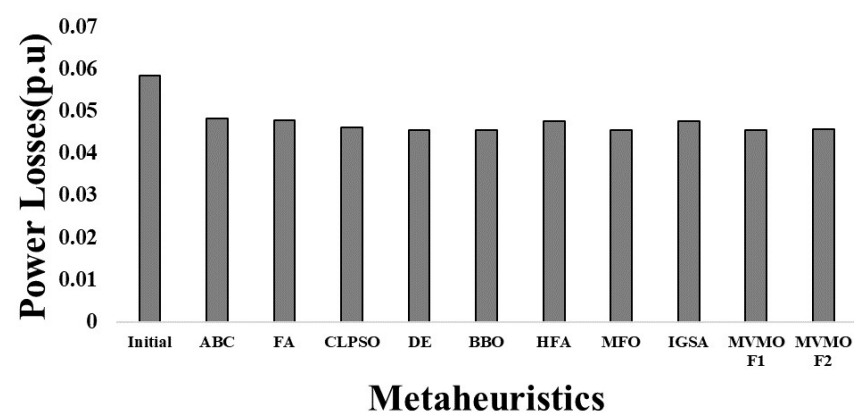


Fig. 4. Comparison of power losses with different metaheuristics techniques for the IEEE 30-bus test system.

Source: Authors.

TABLE 2A. CONTROL VARIABLES FOR POWER LOSS MINIMIZATION WITH DIFFERENT ALGORITHMS (IEEE-30 BUS TEST SYSTEM)

Control variable (pu)	Initial [7]	ABC [19]	FA [19]
V_{G1}	1.05	1.1	1.1
V_{G2}	1.04	1.0615	1.0644
V_{G5}	1.01	1.0711	1.07455
V_{G8}	1.01	1.0849	1.0869
V_{G11}	1.05	1.1	1.0916
V_{G13}	1.05	1.0665	1.099
T_{11}	1.078	0.97	1
T_{12}	1.069	1.05	0.94
T_{15}	1.032	0.99	1
T_{36}	1.068	0.99	0.97
Q_{C10}	0	0.05	0.03
Q_{C12}	0	0.05	0.04
Q_{C15}	0	0.05	0.033
Q_{C17}	0	0.05	0.035
Q_{C20}	0	0.041	0.039
Q_{C21}	0	0.033	0.032
Q_{C23}	0	0.009	0.013
Q_{C24}	0	0.05	0.035
Q_{C29}	0	0.024	0.0142
P_{loss}	0.05833	0.048149	0.047694
DV	0.0097	0	0
DFP	0	0	0

Source: [7], [19].

TABLE 2B. CONTROL VARIABLES FOR POWER LOSS MINIMIZATION WITH DIFFERENT ALGORITHMS (IEEE-30 BUS TEST SYSTEM).

Control variable (pu)	CLPSO [13]	DE [7]	BBO [22]
V_{G1}	1.1	1.1	1.1
V_{G2}	1.1	1.0931	1.0944
V_{G5}	1.0795	1.0736	1.0749
V_{G8}	1.1	1.0736	1.0768
V_{G11}	1.1	1.1	1.0999
V_{G13}	1.1	1.1	1.0999
T_{11}	0.9154	1.0465	1.0435
T_{12}	0.9	0.9097	0.9012
T_{15}	0.9	0.9867	0.9824
T_{36}	0.9397	0.9689	0.9692
Q_{C10}	0.049265	0.05	0.049998
Q_{C12}	0.05	0.05	0.04987
Q_{C15}	0.05	0.05	0.049906
Q_{C17}	0.05	0.05	0.04997
Q_{C20}	0.05	0.04406	0.049901
Q_{C21}	0.05	0.05	0.049946
Q_{C23}	0.05	0.028004	0.038753
Q_{C24}	0.05	0.05	0.049867
Q_{C29}	0.05	0.025979	0.029098
P_{loss}	0.046018	0.045417	0.045435
DV	0.001456	0	0
DFP	0	0	0

Source: [13], [7], [22].

TABLE 2C. CONTROL VARIABLES FOR POWER LOSS MINIMIZATION WITH DIFFERENT ALGORITHMS (IEEE-30 BUS TEST SYSTEM).

Control variable (pu)	HFA [19]	MFO [23]	IGSA [17]
V_{G1}	1.1	1.1	1.081281
V_{G2}	1.05433	1.0943	1.072177
V_{G5}	1.07514	1.0747	1.050142
V_{G8}	1.08688	1.0766	1.050234
V_{G11}	1.1	1.1	1.1
V_{G13}	1.1	1.1	1.068826
T_{11}	0.9801	1.0433	1.08
T_{12}	0.9500	0.9	0.902
T_{15}	0.9702	0.97912	0.99
T_{36}	0.9700	0.96474	0.976
Q_{C10}	0.04700	0.05	0
Q_{C12}	0.04706	0.05	0
Q_{C15}	0.04701	0.04805	0.038
Q_{C17}	0.02306	0.05	0.049
Q_{C20}	0.04803	0.04026	0.0395
Q_{C21}	0.04902	0.05	0.05
Q_{C23}	0.04804	2.5193	0.0275
Q_{C24}	0.04805	0.05	0.05
Q_{C29}	0.03398	0.021925	0.024
P_{loss}	0.04753	0.04541	0.04762
DV	0.0061	0	0
DFP	0	0	0

Source: [19], [23], [17].

TABLE 2D. CONTROL VARIABLES FOR POWER LOSS MINIMIZATION WITH DIFFERENT ALGORITHMS (IEEE-30 BUS TEST SYSTEM).

Control Variable (pu)	MVMO (F_1)	MVMO (F_2)
V_{G1}	1.1	1.09925
V_{G2}	1.094	1.09325
V_{G5}	1.0745	1.07225
V_{G8}	1.07675	1.0745
V_{G11}	1.1	1.0985
V_{G13}	1.1	1.097
T_{11}	1.052	1.038
T_{12}	0.9	0.934
T_{15}	0.984	0.996
T_{36}	0.968	0.977
Q_{C10}	0.05	0.046
Q_{C12}	0.05	0.0415
Q_{C15}	0.05	0.0295
Q_{C17}	0.05	0.047
Q_{C20}	0.043	0.039
Q_{C21}	0.05	0.048
Q_{C23}	0.027	0.041
Q_{C24}	0.05	0.047
Q_{C29}	0.0245	0.0255
P_{loss}	0.045399	0.045626
DV	0	0
DFP	0	0

Source: Authors.

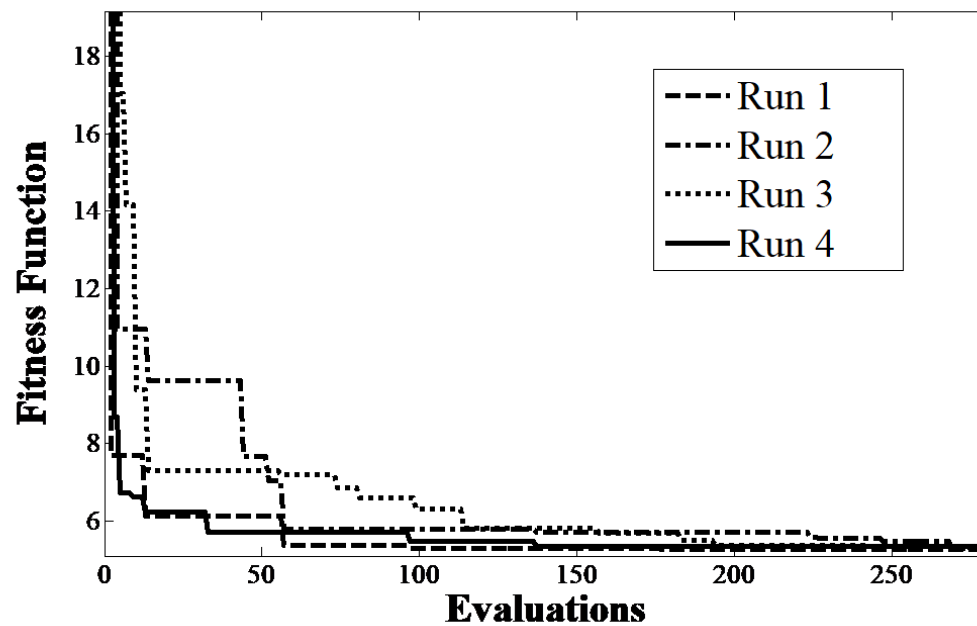


Fig. 5. MVMO convergence with for the IEEE 30-bus test system.
Source: Authors.

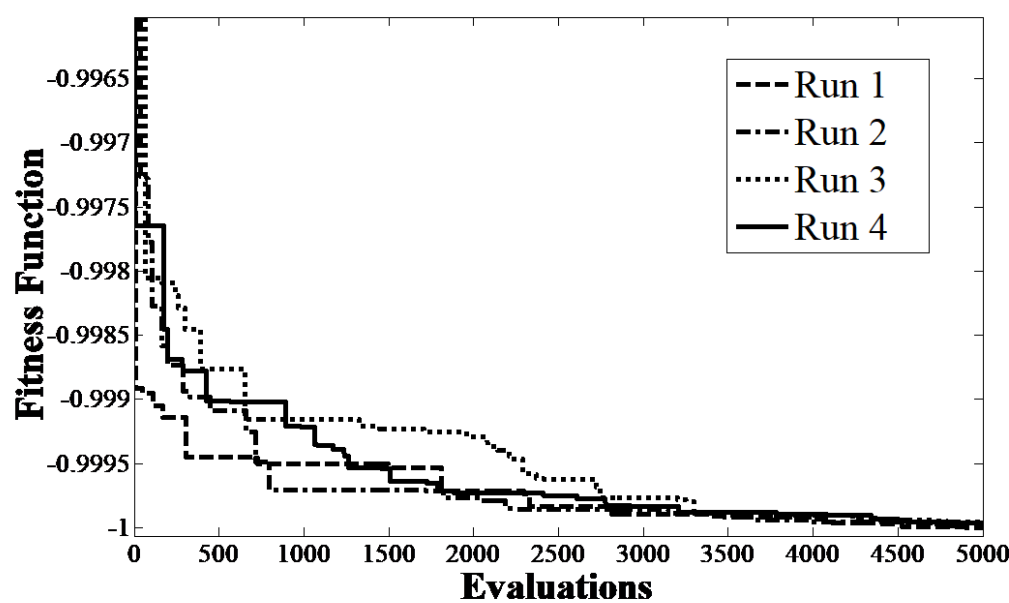


Fig. 6. MVMO convergence with for the IEEE 30-bus test system.
Source: Authors.

C. Results with the IEEE 57-bus test system

Results obtained with the IEEE 57-bus test system are presented in p.u with a 100 MVA base in Table 3a, Table 3b, Table 3c and Table 3d. To guarantee the reproducibility of the results, the values of all the control variables are shown in Table 3a, Table 3b, Table 3c and Table 3d. The power losses before optimization are 27.864 MW (Table 1). After optimization, the maximum reduction in power losses is obtained with the proposed MVMO algorithm when using . In this case, the power losses are 23.81 MW, which represents a reduction of 14.5% with respect to the base case. Note that when applying the fitness function , the MVMO is slightly outperformed by the MFO; however, its performance is still superior to that of the other metaheuristics. Fig. 7 allows comparing the results obtained with the different methodologies. It can be seen that the performance of the MVMO for this power system is similar to that of MFO, and BBO. Fig. 8 and Fig. 9 illustrate the convergence of the proposed approach for the fitness functions and , respectively considering four independent executions.

TABLE 3A. CONTROL VARIABLES FOR POWER LOSS MINIMIZATION WITH DIFFERENT ALGORITHMS (IEEE 57-BUS TEST SYSTEM).

Control Variable (pu)	Initial [7]	SOA [21]	CLPSO [13]
V_{G1}	1.04	1.0541	1.0541
V_{G2}	1.01	1.0529	1.0529
V_{G3}	0.985	1.0337	1.0337
V_{G6}	0.98	1.0313	1.0313
V_{G8}	1.05	1.0496	1.0496
V_{G9}	0.98	1.0302	1.0302
V_{G12}	1.015	1.0302	1.0342
T_{4-18}	0.97	0.99	0.99
T_{4-18}	0.978	0.98	0.98
T_{21-20}	1.043	0.99	0.99
T_{24-26}	1.043	1.01	1.01
T_{7-29}	0.967	0.99	0.99
T_{34-32}	0.965	0.93	0.93
T_{11-41}	0.955	0.91	0.91
T_{15-45}	0.955	0.97	0.97
T_{14-46}	0.9	0.95	0.95
T_{10-51}	0.93	0.98	0.98
T_{13-49}	0.895	0.95	0.95
T_{11-43}	0.958	0.95	0.95
T_{40-56}	0.958	1	1
T_{39-57}	0.98	0.96	0.96
T_{9-55}	0.94	0.97	0.97
Q_{C18}	0	0.0988	0.0988
Q_{C25}	0	0.0542	0.0542
Q_{C53}	0	0.0628	0.0628
P_{loss}	0.2786	0.2487	0.2489
DV	0.7951	0	0
DFP	0.2948	0.0035	0.0022

Source: [7], [21], [13].

TABLE 3B. CONTROL VARIABLES FOR POWER LOSS MINIMIZATION WITH DIFFERENT ALGORITHMS (IEEE 57-BUS TEST SYSTEM).

Control Variable (pu)	BBO [22]	ALC- PSO [14]	MFO [23]
V_{G1}	1.06	1.06	1.06
V_{G2}	1.0504	1.0593	1.0587
V_{G3}	1.044	1.0491	1.0469
V_{G6}	1.0376	1.0432	1.0421
V_{G8}	1.055	1.06	1.06
V_{G9}	1.0229	1.0451	1.0423
V_{G12}	1.0323	1.0411	1.0373
T_{4-18}	0.9669	0.9611	0.95011
T_{4-18}	0.9902	0.9109	1.0076
T_{21-20}	1.012	0.9	1.0063
T_{24-26}	1.0087	0.9004	1.0076
T_{7-29}	0.9707	0.9106	0.97523
T_{34-32}	0.9686	0.9	0.97218
T_{11-41}	0.9008	0.9	0.9

Control Variable (pu)	BBO [22]	ALC- PSO [14]	MFO [23]
T_{15-45}	0.966	0.9	0.97186
T_{14-46}	0.9507	1.0275	0.95355
T_{10-51}	0.9641	0.9876	0.96736
T_{13-49}	0.9246	0.9756	0.92788
T_{11-43}	0.9502	0.9	0.96406
T_{40-56}	0.9966	0.9	0.9998
T_{39-57}	0.9628	1.0121	0.9606
T_{9-55}	0.96	0.9944	0.97899
Q_{C18}	0.09782	0.0994	0.099968
Q_{C25}	0.05899	0.059	0.059
Q_{C53}	0.06289	0.063	0.063
P_{loss}	0.2454	0.2618	0.242529
VD	0	0.1428	0.0000729
DFP	0.00035	0.0829	0

Source: [22], [14], [23].

TABLE 3C. CONTROL VARIABLES FOR POWER LOSS MINIMIZATION WITH DIFFERENT ALGORITHMS (IEEE 57-BUS TEST SYSTEM).

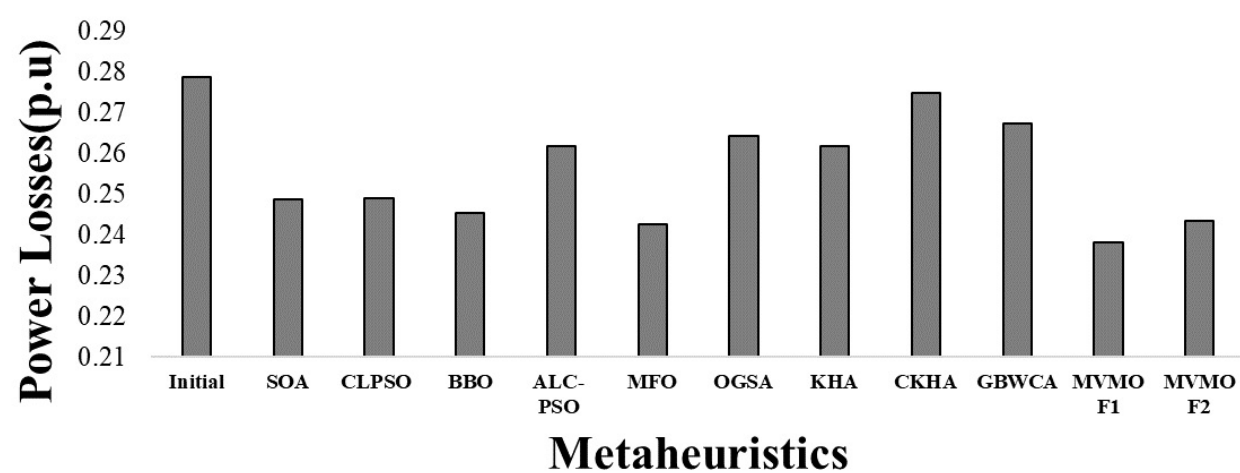
Control Variable (pu)	OGSA [18]	KHA [8]	CKHA [8]
V_{G1}	1.06	1.0556	1.06
V_{G2}	1.0594	1.0595	1.059
V_{G3}	1.0492	1.0414	1.0487
V_{G6}	1.0433	1.0314	1.0431
V_{G8}	1.06	1.0549	1.06
V_{G9}	1.045	1.0415	1.0447
V_{G12}	1.0407	1.0398	1.041
T_{4-18}	0.9	0.9211	0.9179
T_{4-18}	0.9947	1.0214	1.0256
T_{21-20}	0.9	0.9912	0.9
T_{24-26}	0.9001	0.9119	0.902
T_{7-29}	0.9111	0.9101	0.9104
T_{34-32}	0.9	0.9946	0.9005
T_{11-41}	0.9	0.9457	0.9
T_{15-45}	0.9	0.9914	0.9
T_{14-46}	1.0464	1.0714	1.0797
T_{10-51}	0.9875	0.9945	0.9887
T_{13-49}	0.9638	0.9814	0.9914
T_{11-43}	0.9	0.9715	0.9
T_{40-56}	0.9	0.9001	0.9002
T_{39-57}	1.0148	1.0136	1.0173
T_{9-55}	0.983	1.0089	1.0023
Q_{C18}	0.0682	0.0894	0.0994
Q_{C25}	0.059	0.0459	0.059
Q_{C53}	0.063	0.0625	0.063
P_{loss}	0.2642	0.2618	0.2748
VD	0.1036	0.0851	0.0818
PF	0.0948	0.0107	0.1445

Source: [18], [8].

TABLE 3D. CONTROL VARIABLES FOR POWER LOSS MINIMIZATION WITH DIFFERENT ALGORITHMS (IEEE 57-BUS TEST SYSTEM).

Control Variable (pu)	GBWCA [24]	MVMO (F_1)	MVMO (F_2)
V_{G1}	1.06	1.06	1.05945
V_{G2}	1.0591	1.05835	1.05175
V_{G3}	1.0492	1.0457	1.038
V_{G6}	1.0399	1.038	1.03525
V_{G8}	1.0586	1.05835	1.0545
V_{G9}	1.0461	1.04075	1.0336
V_{G12}	1.0413	1.03745	1.0347
T_{4-18}	0.9712	0.929	1.042
T_{4-18}	0.9243	0.955	0.909
T_{21-20}	0.9123	1.008	1.033
T_{24-26}	0.9001	1.006	1.018
T_{7-29}	0.9112	0.939	0.939
T_{34-32}	0.9004	0.973	0.976
T_{11-41}	0.9128	0.9	0.958
T_{15-45}	0.9	0.936	0.929
T_{14-46}	1.0218	0.922	0.917
T_{10-51}	0.9902	0.935	0.967
T_{13-49}	0.9568	0.9	0.922
T_{11-43}	0.9	0.925	0.924
T_{40-56}	0.9	1.007	1.06
T_{39-57}	1.0118	0.975	0.959
T_{9-55}	1	0.94	0.956
Q_{C18}	0.0914	0.092	0.042
Q_{C25}	0.0587	0.059	0.042
Q_{C53}	0.0634	0.063	0.049
P_{loss}	0.2674	0.238113	0.243284
VD	0.3913	0	0
PFD	0.0895	0.000	0.0000

Source: [24].


Fig. 7. Comparison of power losses with different metaheuristics techniques for the IEEE 57-bus test system.

Source: Authors.

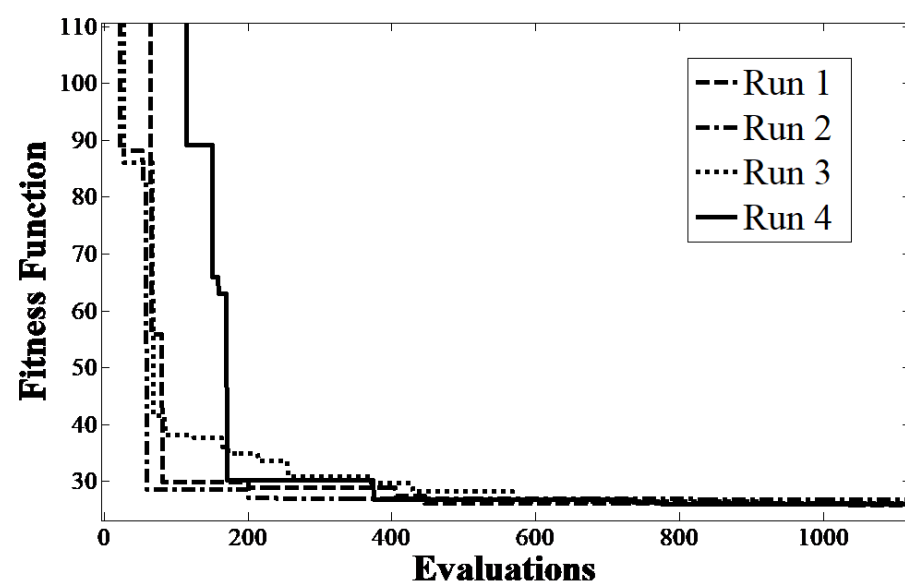


Fig. 8. MVMO convergence with for the IEEE 57-bus test system.
Source: Authors.

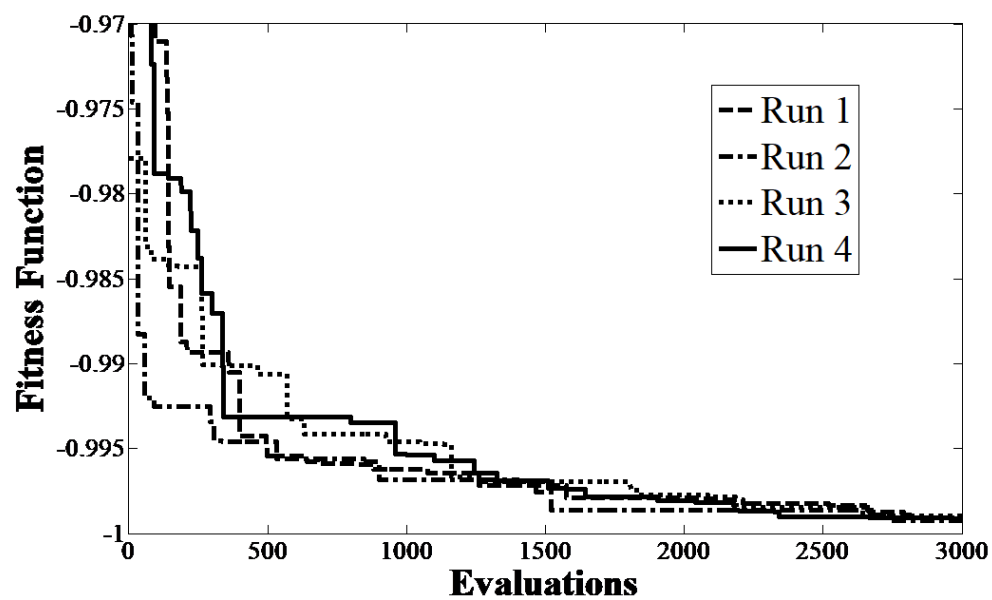


Fig. 9. MVMO convergence with for the IEEE 57-bus test system.
Source: Authors.

D. Performance analysis of the MVMO

Table 4 presents some statistical results of the MVMO performance for 100 runs with the two IEEE power systems under study. Note that better solutions are obtained by implementing a classic penalty (F_1) for both systems. However, this difference is small (0.5% for IEEE 30-bus test system and 2.12% for IEEE 57-bus test system). The main advantage of implementing lies in its shorter calculation time, as can be seen in the last row of Table 4. It should be mentioned that both approaches to managing constraints are effective since the voltage deviations and power flow deviations are zero for both power systems. Furthermore, all the solutions obtained in the runs are very similar, as can be deduced from the standard deviations.

TABLE 4. STATISTICAL RESULTS OF MINIMIZATION OF POWER LOSSES FOR DIFFERENT IEEE POWER SYSTEMS BASED ON 100 RUNS.

IEEE test system	30		57	
Fitness function	F_1	F_2	F_1	F_2
Best solution, MW	4.5399	4.5626	23.8113	24.3284
VD, pu	0	0	0	0
PFD, pu	0	0	0	0
Worst solution, MW	4.5791	4.5700	23.9530	24.4297
Mean, MW	4.5514	4.5684	23.8454	24.4046
Standard Deviation	0.0092	0.0014	0.0275	0.0219
Average computing time (seconds)	1.8917	1.7687	2.6630	1.7363

Source: Authors.

V. CONCLUSIONS

This work presented a novel metaheuristic to solve the problem of optimal reactive power dispatch. The proposed metaheuristic is a stochastic population optimization technique known as MVMO. The distinctive feature of this algorithm is the use of an applied mapping function to mutate new candidate solutions based on the mean and variance of the best population reached. Two different constraint management approaches are applied: a conventional penalty for deviations from feasible solutions and a product of subfunctions that serves to identify when a solution is optimal and feasible. Although slightly better solutions were obtained (0.37% better), with the classic approach of managing constraints; the second one is faster with 35% savings in calculation time, which makes it more suitable for online applications.

The proposed adaptation of the MVMO was found to be able to find better results than previously reported for the IEEE 30 and 57-bus test systems. The values of the control variables are presented so that the results can be verified by researchers for future comparison with other metaheuristics.

ACKNOWLEDGMENTS

The authors would like to acknowledge the sustainability project of Universidad de Antioquia for its support in the development of this project.

REFERENCES

- [1] S. M. Mohseni-Bonab & A. Rabiee, "Optimal reactive power dispatch: a review, and a new stochastic voltage stability constrained multi-objective model at the presence of uncertain wind power generation," *IET Gener Transm Distrib*, vol. 11, no. 4, pp. 815–829, Mar. 2017. <https://doi.org/10.1049/iet-gtd.2016.1545>
- [2] R. Mota-Palomino & V. H. Quintana, "Sparse Reactive Power Scheduling by a Penalty Function - Linear Programming Technique," *IEEE Trans Power Syst*, vol. 1, no. 3, pp. 31–39, Ago. 1986. <https://doi.org/10.1109/TPWRS.1986.4334951>
- [3] K. Aoki, M. Fan, & A. Nishikori, "Optimal VAR planning by approximation method for recursive mixed-integer linear programming," *IEEE Trans Power Syst*, vol. 3, no. 4, pp. 1741–1747, Nov. 1988. <https://doi.org/10.1109/59.192990>
- [4] V. H. Quintana & M. Santos-Nieto, "Reactive-power dispatch by successive quadratic programming," *IEEE Trans Energy Convers*, vol. 4, no. 3, pp. 425–435, Sep. 1989. <https://doi.org/10.1109/60.43245>
- [5] F. C. Lu & Y. Y. Hsu, "Reactive power/voltage control in a distribution substation using dynamic programming," *Transm Distrib IEE Proc - Gener*, vol. 142, no. 6, pp. 639–645, Nov. 1995. <https://doi.org/10.1049/ip-gtd:19952210>
- [6] S. Granville, "Optimal reactive dispatch through interior point methods," *IEEE Trans Power Syst*, vol. 9, no. 1, pp. 136–146, Feb. 1994. <https://doi.org/10.1109/59.317548>
- [7] A. A. A. E. Ela, M. A. Abido, & S. R. Spea, "Differential evolution algorithm for optimal reactive power dispatch," *Electr Power Syst Res*, vol. 81, no. 2, pp. 458–464, Feb. 2011. <https://doi.org/10.1016/j.epsr.2010.10.005>
- [8] A. Mukherjee & V. Mukherjee, "Solution of optimal reactive power dispatch by chaotic krill herd algorithm," *Transm Distrib IET Gener*, vol. 9, no. 15, pp. 2351–2362, 2015. <https://doi.org/10.1049/iet-gtd.2015.0077>
- [9] A. H. Gandomi & A. H. Alavi, "Krill herd: A new bio-inspired optimization algorithm," *Commun Nonlinear Sci Numer Simul*, vol. 17, no. 12, pp. 4831–4845, Dic. 2012. <https://doi.org/10.1016/j.cnsns.2012.05.010>
- [10] H. Yoshida, K. Kawata, Y. Fukuyama, S. Takayama & Y. Nakanishi, "A particle swarm optimization for reactive power and voltage control considering voltage security assessment," presented at *IEEE Power Engineering Society Winter Meeting. Conference Proceedings*, Cat. No.01CH37194, COLO, USA, 2001. <https://doi.org/10.1109/PESW.2001.916897>
- [11] A. A. A. Esmín, G. Lambert-Torres & A. C. Zambroni de Souza, "A hybrid particle swarm optimization applied to loss power minimization," *IEEE Trans Power Syst*, vol. 20, no. 2, pp. 859–866, May. 2005. <https://doi.org/10.1109/TPWRS.2005.846049>
- [12] D. Gutiérrez, W. M. Villa, & J. M. López-Lezama, "Flujo Óptimo Reactivo mediante Optimización por Enjambre de Partículas," *Inf Tecnol*, vol. 28, no. 5, pp. 215–224, 2017. <https://doi.org/10.4067/S0718-07642017000500020>
- [13] K. Mahadevan & P. S. Kannan, "Comprehensive learning particle swarm optimization for reactive power dispatch," *Appl Soft Comput*, vol. 10, no. 2, pp. 641–652, Mar. 2010. <https://doi.org/10.1016/j.asoc.2009.08.038>
- [14] R. P. Singh, V. Mukherjee & S. P. Ghoshal, "Optimal reactive power dispatch by particle swarm optimization with an aging leader and challengers," *Appl Soft Comput*, vol. 29, pp. 298–309, Apr. 2015. <https://doi.org/10.1016/j.asoc.2015.01.006>
- [15] S. Duman, Y. Sönmez, U. Güvenç & N. Yörükeren, "Optimal reactive power dispatch using a gravitational search algorithm," *Transm Distrib IET Gener*, vol. 6, no. 6, pp. 563–576, Jun. 2012. <https://doi.org/10.1049/iet-gtd.2011.0681>

- [16] E. Rashedi, H. Nezamabadi-pour & S. Saryazdi, "GSA: A Gravitational Search Algorithm," *Inf Sci*, vol. 179, no. 13, pp. 2232–2248, Jun. 2009. <https://doi.org/10.1016/j.ins.2009.03.004>
- [17] G. Chen, L. Liu, Z. Zhang, & S. Huang, "Optimal reactive power dispatch by improved GSA-based algorithm with the novel strategies to handle constraints," *Appl Soft Comput*, vol. 50, pp. 58–70, Jan. 2017. <https://doi.org/10.1016/j.asoc.2016.11.008>
- [18] B. Shaw, V. Mukherjee & S. P. Ghoshal, "Solution of reactive power dispatch of power systems by an opposition-based gravitational search algorithm," *Int J Electr Power Energy Syst*, vol. 55, pp. 29–40, Feb. 2014. <https://doi.org/10.1016/j.ijepes.2013.08.010>
- [19] A. Rajan & T. Malakar, "Optimal reactive power dispatch using hybrid Nelder–Mead simplex based firefly algorithm," *Int J Electr Power Energy Syst*, vol. 66, pp. 9–24, Mar. 2015. <https://doi.org/10.1016/j.ijepes.2014.10.041>
- [20] M. Ettappan, V. Vimala, S. Ramesh & V. T. Kesavan, "Optimal reactive power dispatch for real power loss minimization and voltage stability enhancement using Artificial Bee Colony Algorithm," *Microprocess Microsyst*, vol. 76, Jul. 2020. <https://doi.org/10.1016/j.micpro.2020.103085>
- [21] C. Dai, W. Chen, Y. Zhu, & X. Zhang, "Seeker Optimization Algorithm for Optimal Reactive Power Dispatch," *IEEE Trans Power Syst*, vol. 24, no. 3, pp. 1218–1231, Aug. 2009. <https://doi.org/10.1109/TPWRS.2009.2021226>
- [22] A. Bhattacharya & P. K. Chattopadhyay, "Biogeography-Based Optimization for solution of Optimal Power Flow problem," *ECTI*, ECTI-CON2010, CNX, pp. 435–439, May. 2010. Available: <https://ieeexplore.ieee.org/document/5491454>
- [23] R. Ng Shin Mei, M. H. Sulaiman, Z. Mustaffa & H. Daniyal, "Optimal reactive power dispatch solution by loss minimization using moth-flame optimization technique," *Appl Soft Comput*, vol. 59, pp. 210–222, Oct. 2017. <https://doi.org/10.1016/j.asoc.2017.05.057>
- [24] A. A. Heidari, R. Ali Abbaspour & A. Rezaee Jordehi, "Gaussian bare-bones water cycle algorithm for optimal reactive power dispatch in electrical power systems," *Appl Soft Comput*, vol. 57, pp. 657–671, Aug. 2017. <https://doi.org/10.1016/j.asoc.2017.04.048>
- [25] D. Gutierrez Rojas, J. Lopez Lezama & W. Villa, "Metaheuristic Techniques Applied to the Optimal Reactive Power Dispatch: a Review," *IEEE Lat Am Trans*, vol. 14, no. 5, pp. 2253–2263, May. 2016. <https://doi.org/10.1109/TLA.2016.7530421>
- [26] W. M. Villa-Acevedo, J. M. López-Lezama, & J. A. Valencia-Velásquez, "A Novel Constraint Handling Approach for the Optimal Reactive Power Dispatch Problem," *Energies*, vol. 11, no. 9, pp. 1–23, 2018. <https://doi.org/10.3390/en11092352>
- [27] I. Erlich, G. K. Venayagamoorthy & N. Worawat, "A Mean-Variance Optimization algorithm," presented at *IEEE CEC*, CEC, BCN, pp. 1–6, 18-23 Jul. 2010. <https://doi.org/10.1109/CEC.2010.5586027>
- [28] I. Erlich, "Mean-variance mapping optimization algorithm home page," *UDE*, 2018. Available: <https://www.uni-due.de/mvmo/>
- [29] J. L. Rueda & I. Erlich, "Optimal dispatch of reactive power sources by using MVMOs optimization," presented at *IEEE CIASG*, CIASG, SG, 16-19 Apr. 2013. <https://doi.org/10.1109/CIASG.2013.6611495>
- [30] J. C. Cepeda, J. L. Rueda & I. Erlich, "Identification of dynamic equivalents based on heuristic optimization for smart grid applications," *IEEE CEC*, CEC, Bris, QLD, AU, 10-15 Jun. 2012. <https://doi.org/10.1109/CEC.2012.6256493>
- [31] J. L. Rueda & I. Erlich, "Evaluation of the mean-variance mapping optimization for solving multimodal problems," *IEEE SIS*, SIS, SG, 16-19 Apr. 2013. <https://doi.org/10.1109/SIS.2013.6615153>

Daniel Camilo Londoño Tamayo. Universidad de Antioquia. Medellín (Colombia). <https://orcid.org/0000-0002-3589-2622>

Jesús María López Lezama. Universidad de Antioquia. Medellín (Colombia). <https://orcid.org/0000-0002-2369-6173>

Walter Mauricio Villa Acevedo. Universidad de Antioquia. Medellín (Colombia). <https://orcid.org/0000-0002-1466-7266>